Controlling the Cross-Sensitivity of Carbon Nanotube Based Gas Sensors to Water Using Zeolites.

Gwyn. P. Evans,[†] David. J. Buckley,[‡] A. Adedigba,[‡] G.Sankar,[‡] Neal. T. Skipper,[¶,§] and Ivan. P. Parkin[*,‡]

[†]*Department of Security and Crime Science, University College London, 35 Tavistock Sq., London, WC1H 9EZ, United Kingdom*

[‡]*Department of Chemistry, University College London, 20 Gordon St., London, WC1H 0AJ, United Kingdom*

[¶]*Department of Physics and Astronomy, University College London, Gower Street, London WC1E 6BT, United Kingdom*

[§] *London Centre for Nanotechnology, 17-19 Gordon Street, London WC1H 0AH, United Kingdom*

E-mail: i.p.parkin@ucl.ac.uk

Phone: +44 (0)20 7679 4669. Fax: +44 (0)20 7679 7463

Abstract

Carbon nanotube based gas sensors can be used to detect harmful environmental pollutants such as NO_2 at room temperature. Whilst showing promise as low powered, sensitive and affordable monitoring devices, cross-sensitivity of functionalised carbon nanotubes to water vapour often obscures the detection of target molecules. This is a barrier to adoption for monitoring of airborne pollutants due to the varying humidity levels found in real world environments. Zeolites, also known as molecular sieves due to their selective adsorption properties, are used in this work to control the cross-sensitivity of single-walled carbon nanotube (SWCNT) based sensors to water vapour. Zeolites incorporated into the sensing layer are found to reduce interference effects that would otherwise obscure the identification of NO_2 gas, permitting repeatable detection over a range of relative humidities. This significant improvement is found to depend on the arrangement of the SWCNT-zeolite layers in the sensing device, as well as the hydrophilicity of the chosen zeolite.

Keywords

single-walled carbon nanotubes, nanotube network, gas sensor, zeolite, molecular sieve, environmental monitoring, humidity, nitrogen dioxide

1 Introduction

The electrical conductance of a single-walled carbon nanotube (SWCNT) network is sensitive to the adsorption of a wide range of gases and vapours.[1,2] As such, they have been previously used as the active sensing element in chemical sensors, demonstrating a change in network conductivity upon the introduction of a chosen molecule.[3–6]

SWCNT based sensors are low cost and operate at room temperature,[1] permitting the design of low powered and highly portable devices.[7,8] They may be particularly suited to

applications in environmental monitoring, due to their high sensitivity to nitrogen dioxide (NO_2) gas at parts per billion (ppb) concentrations in air.[9,10] Long term exposure to NO_2 has contributed to respiratory disease rates in urban populations. Therefore, affordable monitoring of such pollutants is required to move towards a cleaner, healthier city environment.

Whilst showing promise, carbon nanotube based sensors display a number of undesirable characteristics.[11] One particular barrier to the development of practical devices is the cross-sensitivity of functionalised carbon nanotube sensors to H_2O.[9,12,13] To increase selectivity towards a certain molecule and aid device fabrication, SWCNT samples are often covalently[6,14] or non-covalently[4,15–17] functionalised. After such treatments, a SWCNT based device may display a sizable decrease in conduction upon exposure to H_2O vapour.[18–21] This decrease is much larger than the typical increase in SWCNT network conductance observed when a sensor is exposed to low concentrations of NO_2 gas. Therefore, any variation in the relative humidity of the operating environment can mask and obscure the sensing response (S) of a SWCNT sensor to NO_2, where S is defined as the ratio of device conductance upon gas exposure (G_{Gas}) to its baseline conductance in air (G_{Air}), so that:

$$S = \frac{G_{Gas}}{G_{Air}} \tag{1}$$

and

$$\Delta G = G_{Gas} - G_{Air} \tag{2}$$

where ΔG is the change in conductance induced by exposure to a target gas.

Highly porous metal-organic frameworks (MOFs) and zeolites have been utilised as chemical sensors.[22,23] Mesoporous silica thin films have been used to increase the selectivity of SWCNTs towards NO_2 and exclude polar molecules.[24] In the current study, hydrophilic H-Zeolite-Y or less hydrophilic Silicalite-1 was incorporated into the sensing layer to control the problematic cross-sensitivity of surfactant wrapped thick film SWCNT sensors to H_2O vapour. Using this approach, the room temperature NO_2 sensing properties of SWCNTs

were preserved whilst investigating the effect of zeolite hydrophilicity on sensor responses in humid conditions.

Zeolites are porous alumino-silicate frameworks that demonstrate size and shape selective adsorbance of certain molecules.[25] As zeolites display ionic conductivity (and are usually electrically insulating materials), they have previously been used for impedance based gas sensing,[23] as well as to improve selectivity in a combinatorial approach using metal oxide semiconducting (MOS) gas sensors.[26–28] However, their incorporation into carbon nanotube based sensors has not been investigated previously.

Results indicate that the incorporation of zeolite layers decreases sensitivity to H_2O vapour, with sensors maintaining an increase in conduction upon exposure to 10 parts per million (ppm) of NO_2 gas with varying levels of relative humidity. Conversely, the control SWCNT sensors demonstrate a decrease in network conduction under the same test conditions, with the normal sensing of NO_2 obscured by the presence of H_2O vapour in the test chamber.

In this paper, the zeolites are either deposited over the SWCNT network as a top layer, or SWCNTs are deposited over the zeolite to form a percolating network in a mixed layer. The ordering of the sensing layer is found to greatly affect the sensor response observed to NO_2 in both dry air and humid conditions, with the mixed layer arrangement providing a larger response magnitude.

2 Experimental Section

2.1 Non-covalent Functionalisation of HiPco SWCNTs

SWCNTs produced via the high pressure carbon monoxide disproportionation (HiPco) process[29] (purchased from from Nanointegris, batch number: R1-831) were dried in air at 120°C to remove moisture from the bundles and stored under vacuum. The black powder was added

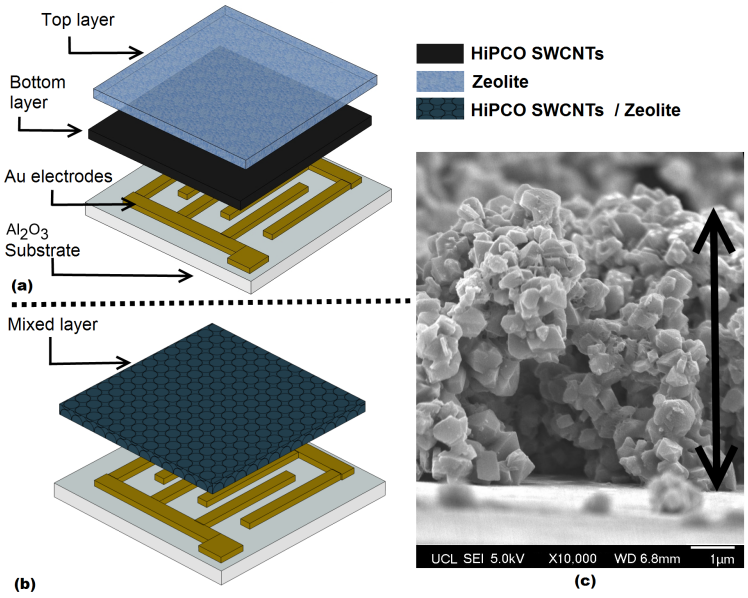

Figure 1: Schematic of a 3 x 3 mm Alumina substrate with interdigitated gold electrodes. Arrangement (a) consists of a HiPco SWCNT base layer with a top layer of porous zeolite. Arrangement (b) represents HiPco SWCNTs deposited over a zeolite to form a mixed layer and (c) a side on SEM micrograph at X10,000 magnification showing a H-Zeolite-Y layer of ≈ 7 μm thickness.

to a solution of deuterated water (D_2O) and sodium deoxycholate (DOC, 2 wt%) at a concentration of approximately 0.5 mg ml^{-1}. DOC is a surfactant molecule that forms micelle like structures around the nanotubes.[30] To aid efficient solubilisation via surfactant wrapping, the solution was sonicated using a 225 W tip sonication probe for 15 minutes, with the container placed in an ice bath for cooling.

The well dispersed solution was centrifuged at 4000g for 30 minutes and the upper 80% of the supernatant was decanted to limit the presence of carbonaceous impurities in the final dispersion.

2.2 Zeolites

Hydrophilic H-Zeolite-Y was obtained from Zeolyst international (product code: CBV600). Less hydrophilic Silicalite-1 was synthesised in house using the method described by Guth *et al.*[31]Both zeolites were then dispersed in ethanol using a magnetic stirrer bar at a con-

centration of 0.2 g ml^{-1}.

2.3 Device Fabrication

A 3 x 3 mm alumina tile with patterned gold electrodes of 175 μm separation (as shown in Figure 1a) was used as the sensor substrate. A single strip (containing 5 individual substrates) was placed in a grooved metal holder (heated to 50°C via hotplate) and the square gold connector pads were covered using a removable mask. The dispersion of HiPco SWCNTs was then deposited across the interdigitated gold electrodes for each of the 5 chips using a calibrated Finnpipette novus electronic single-channel micro pipette (drop volume 1 μL per sensor). The deposition was left to dry for in air for 15 minutes and the substrates were separated into individual chips. This process was repeated to produce 4 batches and 20 individual control HiPco SWCNT sensors.

For each type of top layer sensor, the aforementioned procedure was followed by an additional 1 μL deposition of the dispersed zeolite on top of the SWCNT network, with an extra drying step (Figure 1a). The mixed layer configuration was achieved by depositing the insulating zeolite over the gold electrodes in the same manner as before, drying and depositing 1 μL of the initial HiPco SWCNT solution over the zeolite to form a percolating mixed layer from which an electrical measurement could be made (Figure 1b).

The sensors were then dried in air in a furnace at 100°C for 1 hour. Four of each sensor type (shown in Table 1) were selected from each batch and attached to sensor casings via micro welded platinum wire connections to the gold connector pads.

2.4 Characterisation

A Jeol JSM-6700F field emission scanning electron microscope was used in secondary electron imaging mode to image the zeolite top layers and HiPco zeolite mixed layers using a 5 kV probe voltage at a working distance of 5.9 mm. Samples were gold coated for imaging.

Energy-dispersive X-ray spectroscopy (EDS) analysis was carried out using a Jeol JSM-

6700F and a secondary electron image on a Hitachi S-3400N field emission instrument (15 kV) at a 15 mm working distance, with elemental weight % calculated using the Oxford Instruments INCA software package. Sensors were also gold coated whilst performing EDS measurements.

A Renshaw inVia Raman microscope with laser wavelength 514.5 nm and 1 mW power was used to perform Raman spectroscopy on the surfactant wrapped HiPco DOC solution (deposited on a 3 x 3 alumina substrate before and after heating to 100°C in air).

Attenuated total reflectance - Fourier transform infrared (ATR - FTIR) spectroscopy was performed using a Brucker ALPHA FTIR spectrometer with a diamond crystal and an ATR attachment. Each spectrum was obtained by averaging 64 scans at a resolution of 4 cm^{-1} and measurements were repeated 5 times per sample. To obtain a spectrum after exposure to dry air, 50 ppm NO_2 or 50 ppm NO_2 at 50 % RH, 10 mg of sample was placed into the sensor testing chamber with a flow rate of 1 L min^{-1} for 30 minutes. The sample was then removed from the chamber and the ATR - FTIR spectrum was obtained immediately. A new, identical sample was used for each exposure cycle.

2.5 Gas Testing Procedure

Sensors were placed in ports within a circular testing chamber. The synthetic air flow rate, chamber humidity and gas mixing was controlled using digital mass flow controllers, being delivered at a determined concentration through a central inlet. The circular arrangement of the devices, along with the extraction of gas behind each individual port location, ensures that each sensor is exposed to an equal flow and concentration of gas. A potentiostat setup was used to derive the room temperature sensor conductance throughout the testing run.

Prior to the experiments, dry synthetic air was passed over the sensors for 2 hours to obtain a baseline conductance (G_{Air}) and achieve 0 % relative chamber humidity (confirmed using an internal humidity meter). For repeated testing runs, the relative humidity in the

chamber was maintained at 50 % RH for 1 hour to increase the desorption rate of NO_2 from previous experiments before re-establishing baseline and 0 % RH in dry air for 2 hours.

To first establish the characteristics of the SWCNT sensors and their zeolite modified counterparts, procedure one was used to determine qualitatively the response curves to be expected upon introduction of NO_2, water vapour and a combination of both to the sensor surface (exposure time 200 seconds per pulse). In procedure two, the magnitude and direction of the conductance change due to varying chamber humidity from 0 % to 75 % was quantitatively investigated for each sensor type. Finally, procedure three was used to study the variation in sensor responses to NO_2 in both dry and wet air, as well as to compare sensing results across different fabrication batches. Table S1, S2 and S3 in the supporting information show the complete protocols for testing procedure one, two and three respectively.

3 Results and Discussion

3.1 Material Characterisation

Scanning electron microscopy was used to study the morphology of the zeolite top layers and confirm the presence of SWCNT bundles on the surface of the zeolite mixed layer type sensors. Figure 2(a) and (c) shows the larger particulate dimensions of the Silicalite-1 compared with H-Zeolite-Y layers respectively.

At higher magnification, the SWCNT bundles are visible upon the surface of the zeolite mixed layer configuration sensors. These are distributed over the particulate base layer forming a percolating network, bridging zeolite particles and cracks as shown in Figure 2(b) and (d). Zeolite layer thicknesses was in the approximate range of 5 μm to 10 μm as measured by side on SEM (Figure 1(c)).

In conjunction with SEM, energy dispersive X-ray spectroscopy (EDS) was used to confirm the silicon to aluminum ratio of the Silicalite-1 and H-Zeolite-Y layers investigated,

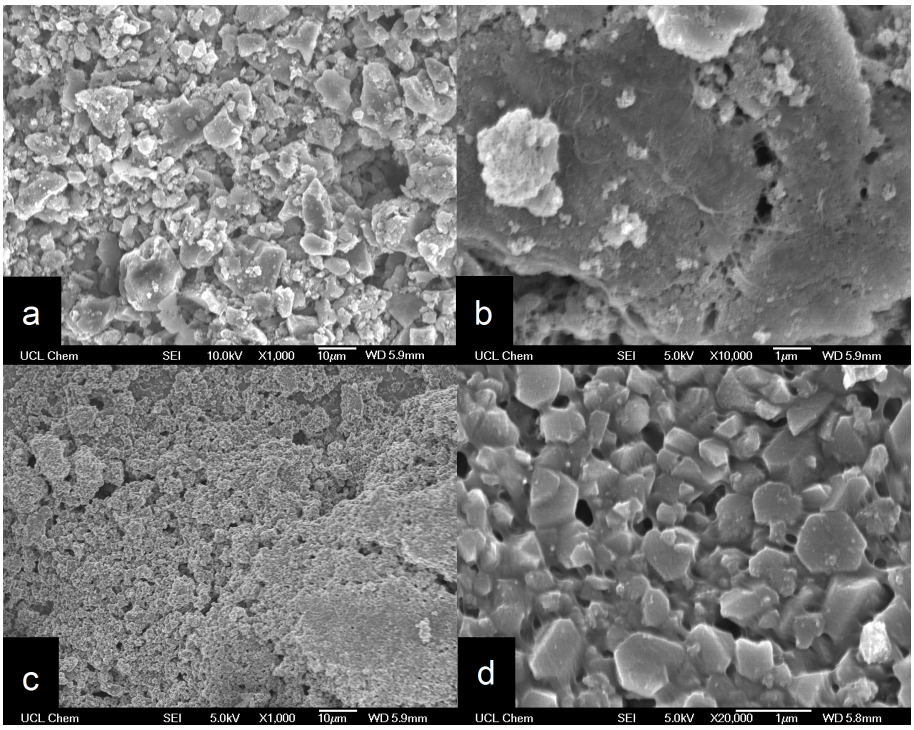

Figure 2: SEM micrographs showing (a) the surface morphology of a Silicalite-1 top layer at X1,000 magnification, (b) bundles of HiPco SWCNTs deposited on a Silicalite-1 to form a mixed layer at X10,000 magnification, (c) the surface morphology of a H-Zeolite-Y top layer at X1,000 magnification and (d) bundles of HiPco SWCNTs deposited on a H-Zeolite-Y to form a mixed layer at X20,000 magnification.

along with the carbon content on the surface of each sensor type. The hydrophobicity of a zeolite depends on its silicon to aluminium framework ratio.[32] Hydrophobic zeolites, such as Silicalite-1, have a high silicon to aluminium framework ratio, whilst the silicon to aluminium ratio of hydrophilic H-Zeolite-Y is low.

As expected, no aluminum was present in the Silicalite-1 sample, where as the H-Zeolite-Y sample had a Si/Al ratio of 3.0 (calculated as the ratio of each elemental % weight), confirming the hydrophilicity of H-Zeolite-Y. No carbon was detected on the surface of the zeolite top layer type sensors, where as the Silicalite-1 and H-Zeolite-Y mixed layer type sensors contained 24% and 21% carbon respectively, corroborating SEM micrograph evidence of carbon nanotube bundles on the mixed layer type sensor surfaces.

Raman spectroscopy measurements provide an indication of residual amorphous carbon and defects in the SWCNT sample before and after heating at 100°C.[33] The ratio of Raman

Table 1: Elemental analysis using energy dispersive X-ray spectroscopy (EDS) to confirm the silicon to aluminum ratio of the Silicalite-1 and H-Zeolite-Y layers investigated (calculated as the ratio of each elemental % weight) along with the Carbon content on the surface of each sensor type. Sensors were gold coated for EDS.

Sensor Type	Surface Carbon content (wt%)	Si:Al Ratio
Silicalite- 1 top layer	0	–
Silicalite-1 mixed layer	24	–
H-Zeolite-Y top layer	0	3
H-Zeolite-Y mixed layer	21	3

intensity of the G peak at 1593 cm^{-1} to the D peak at 1338 cm^{-1} was slightly lower post heating (12.2) than was found for the initial sample (17.2), indicating a possible increase in the number of bundle defects after heat treatment (Figure 3).

3.2 Sensing Results

Many sensing mechanisms for SWCNT sensors have been proposed in the literature.[2,3] It is probable that the exact mechanism depends on nanotube type,[34] defectiveness,[35,36] network density,[37] film thickness,[11,38] device configuration[4,39] and functionalisation technique.[6,15,40–43] With this in mind, sensing results here are described using a mechanism previously applied for sensors based on thick films of SWCNTs that have been functionalised, in conjunction with models describing the characteristics of zeolite layers in gas sensors and possible reactions taking place in the zeolite frameworks.

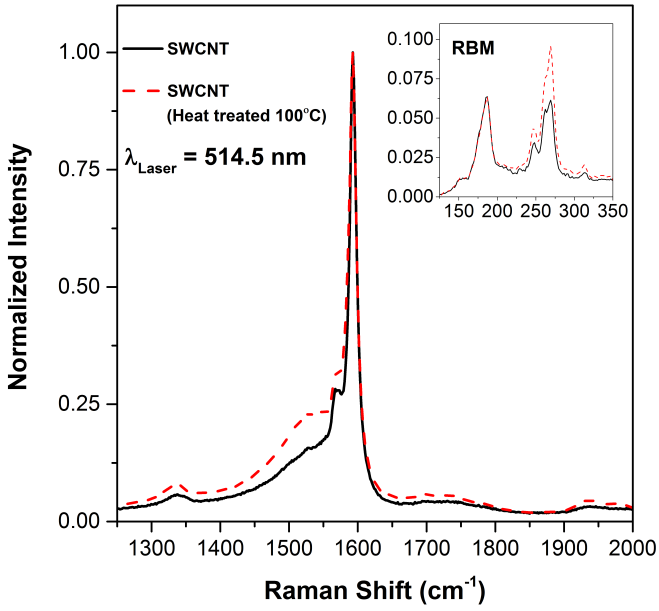

Figure 3: Raman spectra showing the normalized intensity of the D band (1338 cm^{-1}) and G band (1593 cm^{-1}) for HiPco SWCNT DOC bundles before and after heating sample to 100°C, with radial breathing modes inset. G/D ratio before heating was 17.2 and 12.2 after heating, indicating an increase in the number of bundle defects after heat treatment. Laser wavelength $\lambda = 514.5$ nm.

3.3 NO_2 Sensing and H_2O Interference Effects

Under ambient conditions, SWCNT networks exhibit p-type behaviour, due to electron withdrawal of O_2 molecules adsorbed on the tube surfaces.[44,45] The change in conductance for SWCNT network sensors (and thus sensing response), can either be attributed to charge transfer between the target molecule or modulation of the Schottky barrier at semi-conducting nanotube - metallic contacts, depending on the density and metallicity of the SWCNT film.[3,37,46,47]

Testing procedure one was used to qualitatively establish sensing characteristics. Upon exposure to an electron withdrawing molecule, such as NO_2, a p-type increase in conductance is observed as shown in Figure 4 section (b). Alternatively, Figure 4(c) demonstrates that exposure to a species such as H_2O results in a decrease in conductance.

The NO_2 sensing magnitudes and direction of conductance changes are comparable to studies using both functionalised and non-functionalised SWCNT sensors.[1,3,10,18,46,48] Adsorption at nanotube-nanotube junctions is thought to dominate responses in high density nanotube networks, with the degree of metallic SWCNT percolation impacting upon the sensing mechanism.[37,47] Therefore, charge transfer appropriately describes the NO_2 sensing mechanism for the dense, metallic SWCNT networks used in the current study.

Functional groups can also act as interaction sites for gas molecules[14] and it is possible that sensitivity to water vapour is increased after functionalisation of the nanotubes via surfactant wrapping. To investigate this possibility, comparisons were made with previously reported results.

The change in device conductance upon introduction of water vapour is also well documented and often attributed to charge transfer.[18,19] However, responses in the current investigation are found to be larger than studies in which carbon nanotubes were not functionalised. Furthermore, high sensitivity to H_2O and other organic solvents has been observed with functionalised nanotube sensors in previous work, where high sensitivities to water vapour were related to hydrogen bonding or mechanical swelling of the film.[49,50] Therefore, it is suggested that the sensitivity to water vapour observed for the SWCNT control sensors used here is due to interaction of water vapour with both the SWCNT bundles and the functionalising agent.

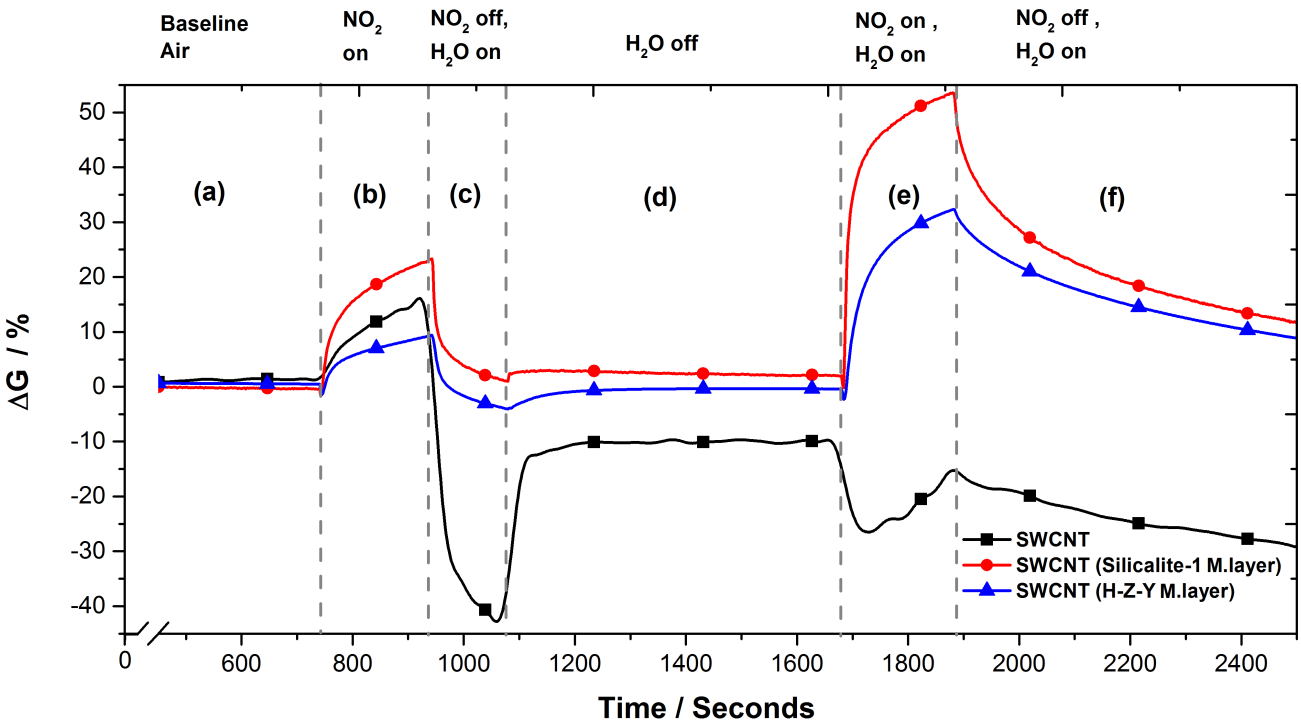

Figure 4: A plot of the typical percentage change in conductance at room temperature (where Δ G = G_{Gas} − G_{Air}) upon exposure to various combinations of NO_2 and H_2O for a blank SWCNT, a SWCNT sensor with a Silicalite-1 mixed layer and a SWCNT sensor with a H-Z-Y mixed layer. Region (a) displays the baseline conductance for each sensor type whilst operating in dry synthetic air, whilst in region (b) 10 ppm of NO_2 is additionally introduced to the testing chamber. Region (c) contains the desorption step in which the NO_2 pulse is turned off and H_2O is turned on resulting in a relative humidity of 75 % inside the testing chamber, aiding NO_2 desorption from the sensor surface. In region (d) H_2O is turned off to return the relative humidity of the chamber to 0 % and recover baseline conductance. Region (e) shows the response of each sensor type to 10 ppm of NO_2 whilst operating at 75 % chamber humidity. Finally, in region (f) the NO_2 is turned off and relative humidity set at 75 % for the desorption cycle.

Whilst this additional mechanism requires further investigation, results here and elsewhere indicate that competing processes take place upon adsorption of NO_2 and H_2O, producing a convoluted response curve. When both NO_2 and H_2O are introduced at step (e) so that the testing chamber humidity is increased from 0 % to 75 %, the detection of NO_2 is masked by H_2O interference for the control SWCNT sensor. This unwanted by-product of functionalisation can be negated through incorporation of zeolites, as is now discussed.

3.4 Reducing Cross-Sensitivity to H_2O

The complex behaviour of the zeolite modified SWCNT sensors can be explained by considering the combined effects of gas diffusion through the zeolite layers, as well as specific interactions between NO_2, H_2O and the chosen zeolite. Firstly, the results of the mixed layer sensor type are described as this configuration provided the most promising results in terms of H_2O interference reduction.

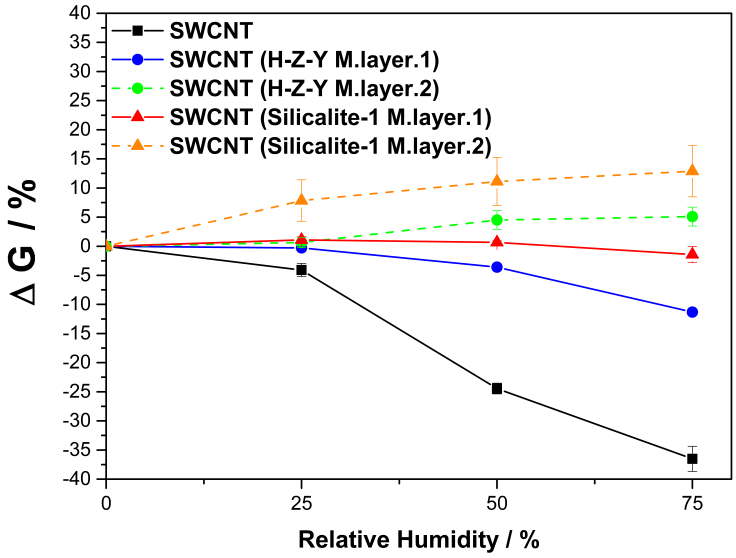

Figure 5: Typical percentage change in conductance per sensor type (where Δ G = G_{Gas} − G_{Air}) as relative humidity in testing chamber is increased from 0 % to 25 %, 50 % and 75 % for SWCNT control sensors, SWCNT H-Zeolite-Y and SWCNT Silicalite-1 zeolite mixed layer type sensors. M.layer.1 indicates a mixed layer with lower zeolite content (0.033 mg of zeolite per 1 μL drop of HiPco DOC solution), M.layer.2 indicates a mixed layer with higher zeolite content (0.2 mg of zeolite per 1 μL drop of HiPco DOC solution).

3.5 Zeolite Mixed Layers

Figure 4 section (c), obtained following testing procedure one, highlights the decreased sensitivity to changing environmental humidity for the SWCNT mixed layer type sensors in comparison with the control. Here, hydrolysis treatment at step (c) removes the NO_2[18]

introduced in step (b), with recovery of the initial baseline resistance. The control SWCNT sensor overshoots its initial baseline resistance, settling at a new value in dry air at step (d), indicating permanent modification of the film. We propose that the SWCNT network deposited over a zeolite is effectively exposed to a lower concentration of water vapour due to adsorption of the H_2O in the zeolite framework.

It was expected here that zeolites with high aluminium content (such as H-Zeolite Y used here) would show a large affinity for water,[32] preferentially adsorbing it over the SWCNT network and reducing interference effects. However, a reduction in sensitivity to H_2O vapour was also observed in the Silicalite-1 mixed layer sensor. Despite the hydrophobic nature of Silicalite-1, water adsorption is still thought to take place due to the presence of silanol defects.[51] This may explain the overall reduction in water interference despite the use of both a hydrophobic (Silicalite-1) and hydrophilic (H-Zeolite-Y) zeolite type. In a similar way, Battie *et al* found that silanol groups permitted the use of mesoporous silica thin films to reduce the cross-sensitivity of SWCNT based devices to water.[24] Therefore, it is more appropriate to refer to the Silicalite-1 used here as being less hydrophilic than H-Zeolite-Y, rather than being hydrophobic.

Figure 5 shows that the device conductance change in humid conditions is dependent on the zeolite loading. Use of a zeolite mixed layer reduces the decrease in conduction when compared to SWCNT control devices. Interestingly, at higher zeolite loadings a comparatively small conductance increase is observed. This may be due to the introduction of water-zeolite reaction products to the nanotube network.

Detection of 10 ppm NO_2 at 75 % relative humidity with the zeolite mixed layer sensors is shown in Figure 4 step (e). Initially, the response magnitude was larger when testing in humid conditions, possibly due to a reaction between the zeolite adsorbed H_2O and NO_2. This feature was found to vary between test cycles, potentially due to different levels of residual H_2O present in the zeolite framework between tests. Therefore, after establishing that a zeolite mixed layer reduces H_2O interference, procedure three was adopted (as out-

lined in the Gas Testing Procedure section) to establish the extent to which responses were reproducible and quantitatively asses the apparent improvements.

Figure 6 shows the collated responses for each sensor type to 10 ppm NO_2 in both synthetic dry air and wet air at 75 % relative humidity (using testing procedure 3). The responses of four identical sensors (one taken from each batch, see device fabrication section) are averaged over six testing cycles to provide a mean response direction and magnitude per sensor type.

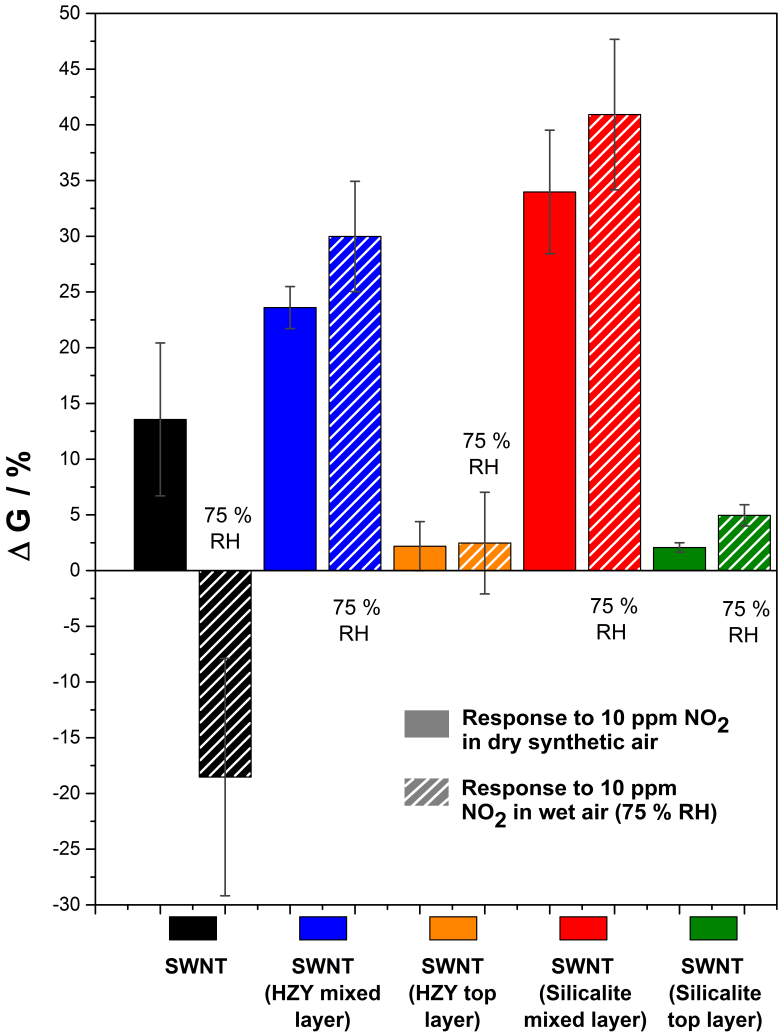

Figure 6: Average percentage change in conductance per sensor type (where Δ G = G_{Gas} − G_{Air}) upon exposure to both 10 ppm NO_2 in dry synthetic air and 10 ppm NO_2 in wet air at 75 % relative humidity over 6 testing cycles (mean responses of four identical sensors from each sensor type, taken over six repeated tests, presented with standard error).

Typically, SWCNT control sensors displayed an increase in conductance of +13.6 % to 10 ppm NO_2 in dry air and a decrease of -18.53 % in wet air (75 % RH), showing a difference in response direction and a 38.3 % difference in G_{Gas}. Whilst the SWCNT control sensors always displayed a decrease in conduction upon introduction of H_2O vapour and NO_2, the magnitude of the response between identical sensors was variable. Variability in SWCNT based sensor performance has been investigated previously and can be attributed to the different properties (length, diameter, semi-conducting or metallic conductivity) of SWCNTs found within a sample[34,52] and thus in the network forming the sensing layer.

Zeolite mixed layer sensors maintain a repeatable overall increase in conductance for NO_2 in both dry and wet air. The increase for H-Zeolite-Y mixed layers is smaller for NO_2 in dry air (+24%) than in wet air (+30%). The average response to NO_2 for Silicalite-1 mixed layer sensors was also lower in dry air (+34%) than in wet (+40.9%), although overall responses were larger in magnitude using Silicalite-1. Here, the differences between the H-Zeolite-Y and Silicalite-1 mixed layer sensors may be due to their different silicon to aluminium ratios. Zeolite water content can dramatically influence the reaction products present inside the framework.[53] As H-Zeolite-Y has a higher affinity for H_2O, it is possible that varying amounts of reaction products are produced that subsequently interact with the SWCNTs.

Attenuated total reflectance - Fourier transform infrared (ATR - FTIR) spectroscopy was used to infer possible reactions taking place in the zeolite framework upon adsorption of NO_2. Any products of reactions between NO_2, H_2O and the acidic sites within the framework can interact and contribute to a change in conductance of the sensing layer. Adsorption of NO_2 in the presence of water by Zeolite-Y type zeolites has been investigated previously using FTIR spectroscopy and was found to inhibit the formation of NO^+ species, whilst NO_3^- and NO_2^- are readily formed, as well as potential HNO_x molecules.[53–55]

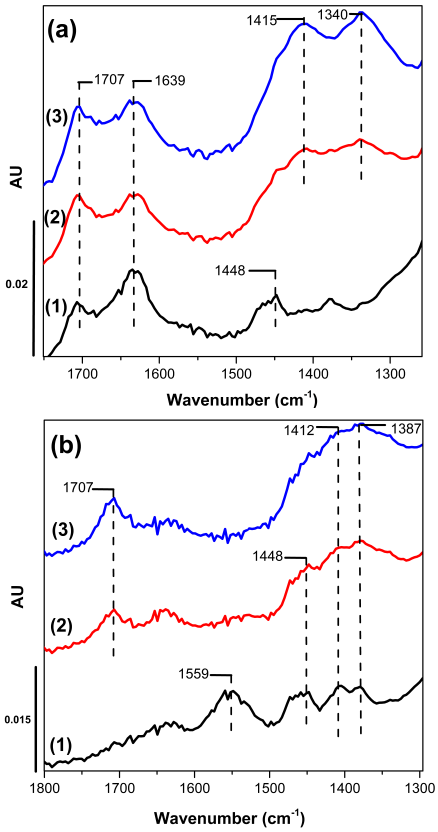

Figure 7: ATR - FTIR spectra for the (a) HiPco SWCNT H-Zeolite-Y sample (b) HiPco SWCNT Silicalite-1 sample when exposed to (1) dry air for 30 minutes (2) 50 ppm NO_2 in dry air for 30 minutes and (3) 50 ppm NO_2 in wet air for 30 minutes at 50 % RH, transferring the samples to the spectrometer after exposure. A Brucker ALPHA FTIR spectrometer with a diamond crystal and an ATR attachment was used, averaging 64 scans at a resolution of 4 cm^{-1}. Five repeated measurements were made per exposure cycle on each sample type, plots are offset for clarity.

Whilst our experimental setup differed from that of the previous study to suit the detection of species in ambient conditions (see experimental section), similar spectral features were observed when exposing a mixed HipCo SWCNT / H-Zeolite-Y sample to 50 ppm NO_2 in either dry or wet air and subsequently obtaining the ATR-FTIR spectra.[53,54] Figure 7a shows the appearance of two bands in the 1300 to 1450 cm^{-1} region after exposing the mixed sample to 50 ppm NO_2 for 30 minutes. An increase in peak intensity is observed when NO_2 is introduced in humid conditions (50 % RH). These bands have been assigned to nitrate groups in the literature, suggesting the formation of HNO_x or NO_3^- species when the zeolite is exposed to NO_2.[53–55]

Similar features are observed in the mixed HiPco SWCNT / Silicalite-1 sample (Figure 7b). The band at 1387 cm^{-1} increases in intensity after adsorption of NO_2 and a further increase is found when adsorption takes place in the presence of water. Furthermore, the band centered at 1559 cm^{-1} in the non-exposed sample disappears after the introduction of NO_2 to the chamber and a new band is formed at 1707 cm^{-1}, suggesting the formation of new surface species. It has been previously reported that nitric acid treatment increases the conductance of SWCNT networks.[56,57] Therefore, the formation of such species (especially HNO_x molecules) within the sensing layers may be causing the larger responses to NO_2 in humid conditions.

The zeolites within the sensing layer have a limited water adsorption capacity. After 10 cycles of testing for the Silicalite-1 mixed layer type sensors and after 7 cycles for the H-Zeolite-Y mixed layer sensors, water starts to interfere with the sensing responses to 10 ppm NO_2 at 75% relative humidity in the testing chamber. Whilst this adds weight to the hypothesis that cross-sensitivity reduction is due to zeolite water adsorption, it also means that the sensor needs to be regenerated periodically in some way to limit zeolite saturation. Figures S3a and S3b in the supporting information show an example of regenerating the mixed layer sensors after multiple testing cycles by heating them to 150°C in air on chip. After this step, the zeolites once again facilitate a reduction in cross-sensitivity to water and responses to NO_2 in humid conditions at room temperature are recovered.

Surprisingly, the H-Zeolite-Y and Silicalite-1 mixed layer sensors show a significantly larger change in conductance upon exposure to 10 ppm NO_2 in dry air than the control SWCNT sensors (24 %, 34 % and 13.6 % respectively, Figure 6). This can be reasoned by considering two contributing factors. Firstly, the conversion of NO_2 to other oxidising products in the vicinity of the tube network may still take place if there is residual water in the zeolite framework, inducing larger responses. Secondly, the proportion of the sensing layer that is accessible to the target gas has previously been shown to impact greatly upon the response observed for nanomaterial based sensors.[11,23] Therefore, the increase may be

partly due to the fact that the SWCNTs are distributed over the highly porous mixed layer, allowing NO_2 gas access to a higher proportion of the SWCNT network, resulting in a higher percentage change in film conductance.

P-type responses to NH_3 were observed using the zeolite mixed layer sensors as detailed in the supporting information. Response magnitudes ($\Delta G < 1$ % to 40 ppm NH_3) were small and the zeolites were unable to provide adequate water interference reduction in this case. However, this may be possible when testing for higher concentrations of NH_3 (200 ppm +) that cause larger changes in the conductance of SWCNT networks.

3.6 Zeolite Top Layers

A profound difference in sensing characteristics is observed between devices utilising a top layer or mixed layer of zeolite, which is attributed to contrasting diffusion processes.[58]

The use of a zeolite layer on top of the sensor introduces a porous barrier to adsorption of NO_2 in the SWCNT network. Thus, a resistive diffusion process seems to limit access of the gas to the functional sensing layer and responses are largely reduced to 10 ppm NO_2 as compared with the SWCNT control and zeolite mixed layer sensors. Interestingly, when 10 ppm of NO_2 is introduced whilst increasing the relative chamber humidity to 75 %, a larger response to NO_2 is observed for the Silicalite-1 top layer sensor.

This difference in sensing response whilst operating in high relative humidities can be attributed to the blocking of NO_2 adsorption sites with water. The wetting of the zeolite framework reduces the layers diffusive resistance, allowing more NO_2 access to the sensing layer. As before, it is also possible that reactions occur in the zeolite layer between NO_2 and adsorbed H_2O, introducing new products to the film.

Mixed layers of zeolite provide an enhanced response magnitude when compared to top layered sensors. This can again be explained when considering the access of the target molecule to the SWCNT network. In the mixed layer configuration, there is less of a dif-

fusive barrier to gas interaction with the SWCNTs. Therefore a higher proportion of the NO_2 gas, as well as subsequent reaction products, interact with the SWCNTs, resulting in a larger electrical response.

3.7 Sensing Characteristics

Response time t_{90}, defined as the time required for sensor responses to reach 90 % of their maximum value (available in Table S4 in the supporting information), varied depending on the sensor type and analyte under investigation. Generally, responses to H_2O (75 % RH) were fastest for the SWCNT control sensors (12 seconds) compared with zeoilte modified sensors (200 to 350 seconds depending on zeolite), presumably as SWCNT exposure to water in the zeolite containing samples is hindered by adsorption to the framework. Baseline conductance was re-established after exposure to water within 200 seconds for all sensors, although some drift was evident as shown in Figure S1 in the supporting information, possibly due to retention of water in the film.

When testing to NO_2 in dry air, response times were of the order of 500 seconds other than for the Silicalite-1 mixed layer type sensor for which t_{90} = 163 seconds. Interestingly, the H-Zeolite-Y mixed layer sensor response time for NO_2 at 75 % RH was faster (341 seconds) than when testing in dry air. This was not the case for the remaining sensors, for which simultaneous exposure to NO_2 and H_2O increased response times (see Table S4, supporting information). Therefore, response times to NO_2 are sensitive to adsorption of water in the zeolite modified sensors. Some baseline drift was evident after exposure to NO_2 (shown in Figure S2 in the supporting information), with stability of responses indicated by the error bars on Figure 6.

4 Conclusion

Zeolite layers have been shown to modify the sensing characteristics of functionalised SWCNTs. The room temperature sensor behaviour, when exposed to NO_2 in both dry and humid conditions, was found to depend on the arrangement of the layers in the device, the loading and hydrophilicity of the chosen zeolite.

The zeolite mixed layer configuration was found to limit cross sensitivity to water vapour, with sensors maintaining an increase in conduction upon exposure to NO_2 in both dry and humid conditions. Furthermore, the difference in response when testing to NO_2 in dry and wet air (S_{DryAir} - $S_{RH\ 75\%}$) was 6.9 % for the SWCNT Silicalite-1 mixed layer sensor type, compared to 32.1 % for the SWCNT control sensors. This desirable reduction of water vapour interference is attributed to the preferential adsorption of H_2O to the zeolite framework rather than to the SWCNTs.

ATR-FTIR measurements indicate the formation of NO_3^- and HNO_3 species in the mixed layer material after exposure to NO_2, which in turn depends on the amount of water present in the zeolite framework. It is suggested that differences in the responses between SWCNT H-Zeolite-Y and SWCNT Silicalite-1 mixed layer sensors are therefore due to their different respective hydrophilicities.

Zeolite top layers were found to inhibit the diffusion of NO_2 to the active SWCNT sensing layer. Thus, the change in conductance observed whilst testing in dry air was relativity low at 2.1 %, with a moderate increase in humid conditions to 5.0 %. A reduced layer thickness ($< 10\ \mu$m) may be required to allow diffusion of the target gas to the SWCNTs in the zeolite top layer sensor arrangement.

These promising results suggest that a mixed sensing layer of SWCNTs and zeolite reduces the cross sensitivity of functionalised SWCNT sensors to water vapour. This is favourable for real world monitoring of NO_2 at room temperature with SWCNT based devices.

Acknowledgement

The authors thank Dr. Steve Firth for instrumentation assistance. This work was carried out under EPSRC Grant no: EP/G037264/1 as part of UCL's Security Science Doctoral Training Centre.

Supporting Information Available

The following files are available free of charge.

Tables detailing the steps and conditions for each sensor testing procedure are supplied in the supporting information. Real time sensor responses to changes in humidity and NO_2 gas in dry and wet air are also provided, along with examples of sensor regeneration.

References

(1) Li, J.; Lu, Y.; Ye, Q.; Cinke, M.; Han, J.; Meyyappan, M. Carbon Nanotube Sensors for Gas and Organic Vapor Detection. *Nano Lett.* **2003**, *3*, 929–933.

(2) Kauffman, D.; Star, A. Carbon Nanotube Gas and Vapor Sensors. *Angew. Chem. Int. Ed.* **2008**, *47*, 6550–6570.

(3) Snow, E. S.; Perkins, F. K.; Robinson, J. A. Chemical Vapor Detection Using Single-walled Carbon Nanotubes. *Chem. Soc. Rev.* **2006**, *35*, 790–798.

(4) Zhang, T.; Mubeen, S.; Myung, N. V.; Deshusses, M. A. Recent Progress in Carbon Nanotube-based Gas Sensors. *Nanotechnology* **2008**, *19*, 332001.

(5) Novak, J. P.; Snow, E. S.; Houser, E. J.; Park, D.; Stepnowski, J. L.; McGill, R. A. Nerve Agent Detection Using Networks of Single-walled Carbon Nanotubes. *Appl. Phys. Lett.* **2003**, *83*, 4026–4028.

(6) Schnorr, J. M.; van der Zwaag, D.; Walish, J. J.; Weizmann, Y.; Swager, T. M. Sensory Arrays of Covalently Functionalized Single-Walled Carbon Nanotubes for Explosive Detection. *Adv. Funct. Mater.* **2013**, 5285–5291.

(7) Llobet, E. Gas Sensors Using Carbon Nanomaterials: A Review. *Sens. Actuators, B* **2013**, *179*, 32–45.

(8) Abraham, J. K.; Philip, B.; Witchurch, A.; Varadan, V. K.; Reddy, C. C. A Compact Wireless Gas Sensor Using a Carbon Nanotube/PMMA Thin Film Chemiresistor. *Smart Mater. Struct.* **2004**, *13*, 1045–1049.

(9) Goldoni, A.; Larciprete, R.; Petaccia, L.; Lizzit, S. Single-Wall Carbon Nanotube Interaction with Gases: Sample Contaminants and Environmental Monitoring. *J. Am. Chem. Soc.* **2003**, *125*, 11329–11333.

(10) Valentini, L.; Armentano, I.; Kenny, J. M.; Cantalini, C.; Lozzi, L.; Santucci, S. Sensors for Sub-ppm NO2 Gas Detection Based on Carbon Nanotube Thin Films. *Appl. Phys. Lett.* **2003**, *82*, 961–963.

(11) Snow, A.; Perkins, F.; Ancona, M.; Robinson, J.; Snow, E.; Foos, E. Disordered Nanomaterials for Chemielectric Vapor Sensing: A Review. *IEEE Sens. J.* **2015**, *15*, 1301–1320.

(12) Cantalini, C.; Valentini, L.; Armentano, I.; Lozzi, L.; Kenny, J. M.; Santucci, S. Sensitivity to NO2 and Cross-sensitivity Analysis to NH3, Ethanol and Humidity of Carbon Nanotubes Thin Film Prepared by PECVD. *Sens. Actuators, B* **2003**, *95*, 195–202.

(13) Zahab, A.; Spina, L.; Poncharal, P.; MarliÃÍre, C. Water-vapor Effect on the Electrical Conductivity of a Single-walled Carbon Nanotube Mat. *Phys. Rev. B* **2000**, *62*, 10000–10003.

(14) Bekyarova, E.; Davis, M.; Burch, T.; Itkis, M. E.; Zhao, B.; Sunshine, S.; Haddon, R. C. Chemically Functionalized Single-Walled Carbon Nanotubes as Ammonia Sensors. *J. Phys. Chem. B* **2004**, *108*, 19717–19720.

(15) Frazier, K. M.; Swager, T. M. Robust Cyclohexanone Selective Chemiresistors Based on Single-Walled Carbon Nanotubes. *Anal. Chem.* **2013**, *85*, 7154–7158.

(16) Lee, C.; Sharma, R.; Radadia, A.; Masel, R.; Strano, M. On-Chip Micro Gas Chromatograph Enabled by a Noncovalently Functionalized Single-Walled Carbon Nanotube Sensor Array. *Angew. Chem. Int. Ed.* **2008**, *47*, 5018–5021.

(17) Liu, S. F.; Lin, S.; Swager, T. M. An Organocobalt-Carbon Nanotube Chemiresistive Carbon Monoxide Detector. *ACS Sensors* **2016**, 354–357.

(18) Randeniya, L. K.; Martin, P. J. Removal of Strongly-bound Gases from Single-walled Carbon Nanotubes without Annealing or Ultraviolet Light Exposure. *Carbon* **2013**, *60*, 498–505.

(19) Randeniya, L.; Bendavid, A.; Martin, P.; Kumar, S. SWCNT-aminopolymer Composites on Mesoporous Alumina for Fast, Room-temperature Detection of Ultra-low Concentrations of NO2 by Mediation of Water Vapour. *Sens. Actuators, B* **2015**, *220*, 1105–1111.

(20) Na, P. S.; Kim, H.; So, H.-M.; Kong, K.-J.; Chang, H.; Ryu, B. H.; Choi, Y.; Lee, J.-O.; Kim, B.-K.; Kim, J.-J.; Kim, J. Investigation of the Humidity Effect on the Electrical Properties of Single-walled Carbon Nanotube Transistors. *Appl. Phys. Lett.* **2005**, *87*, 093101.

(21) Safari, S.; van de Ven, T. G. Effect of Water Vapor Adsorption on Electrical Properties of Carbon Nanotube/Nanocrystalline Cellulose Composites. *ACS Appl. Mater. Interface* **2016**, 9483–9489.

(22) Kreno, L. E.; Leong, K.; Farha, O. K.; Allendorf, M.; Van Duyne, R. P.; Hupp, J. T. Metal–Organic Framework Materials as Chemical Sensors. *Chem. Rev.* **2012**, *112*, 1105–1125.

(23) Sahner, K.; Hagen, G.; Schonauer, D.; Reis, S.; Moos, R. Zeolites-Versatile Materials for Gas sSensors. *Solid State Ionics* **2008**, *179*, 2416–2423.

(24) Battie, Y.; Ducloux, O.; Patout, L.; Thobois, P.; Loiseau, A. Selectivity Enhancement Using Mesoporous Silica Thin Films for Single Walled Carbon Nanotube Based Vapour Sensors. *Sens. Actuators, B* **2012**, *163*, 121–127.

(25) Wales, D. J.; Grand, J.; Ting, V. P.; Burke, R. D.; Edler, K. J.; Bowen, C. R.; Mintova, S.; Burrows, A. D. Gas Sensing Using Porous Materials for Automotive Applications. *Chem. Soc. Rev.* **2015**, *44*, 4290–4321.

(26) Peveler, W. J.; Binions, R.; Hailes, S. M. V.; Parkin, I. P. Detection of Explosive Markers Using Zeolite Modified Gas Sensors. *J. Mater. Chem.A* **2013**, *1*, 2613–2620.

(27) Tarttelin, P.; Naik, A. J. T.; Newton, E. J.; Hailes, S. M. V.; Parkin, I. P. Assessing the Potential of Metal Oxide Semiconducting Gas Sensors for Illicit Drug Detection Markers. *J. Mater. Chem.A* **2014**, 8952–8960.

(28) Pugh, D. C.; Newton, E. J.; Naik, A. J. T.; Hailes, S. M. V.; Parkin, I. P. The Gas Sensing Properties of Zeolite Modified Zinc Oxide. *J. Mater. Chem.A* **2014**, 4758–4764.

(29) Nikolaev, P.; Bronikowski, M. J.; Bradley, R. K.; Rohmund, F.; Colbert, D. T.; Smith, K. A.; Smalley, R. E. Gas-phase Catalytic Growth of Single-walled Carbon Nanotubes from Carbon Monoxide. *Chem. Phys. Lett.* **1999**, *313*, 91–97.

(30) Wenseleers, W.; Vlasov, I. I.; Goovaerts, E.; Obraztsova, E. D.; Lobach, A. S.; Bouwen, A. Efficient Isolation and Solubilization of Pristine Single-Walled Nanotubes in Bile Salt Micelles. *Adv. Funct. Mater.* **2004**, *14*, 1105–1112.

(31) Guth, J. L.; Kessler, H.; Wey, R. New Route to Pentasil-Type Zeolites Using a Non Alkaline Medium in the Presence of Fluoride Ions. **1986**, *28*, 121–128.

(32) Bushuev, Y. G.; Sastre, G.; de Julian-Ortiz, J. V.; Galvez, J. Water–Hydrophobic Zeolite Systems. *J. Phys. Chem. C* **2012**, *116*, 24916–24929.

(33) Dresselhaus, M. S.; Dresselhaus, G.; Saito, R.; Jorio, A. Raman Spectroscopy of Carbon Nanotubes. *Phys. Rep.* **2005**, *409*, 47–99.

(34) Lee, B. Y.; Sung, M. G.; Lee, J.; Baik, K. Y.; Kwon, Y.-K.; Lee, M.-S.; Hong, S. Universal Parameters for Carbon Nanotube Network-Based Sensors: Can Nanotube Sensors Be Reproducible? *ACS Nano* **2011**, *5*, 4373–4379.

(35) Robinson, J. A.; Snow, E. S.; Badescu, S. C.; Reinecke, T. L.; Perkins, F. K. Role of Defects in Single-Walled Carbon Nanotube Chemical Sensors. *Nano Lett.* **2006**, *6*, 1747–1751.

(36) Salehi-Khojin, A.; Khalili-Araghi, F.; Kuroda, M. A.; Lin, K. Y.; Leburton, J.-P.; Masel, R. I. On the Sensing Mechanism in Carbon Nanotube Chemiresistors. *ACS Nano* **2011**, *5*, 153–158.

(37) Boyd, A.; Dube, I.; Fedorov, G.; Paranjape, M.; Barbara, P. Gas Sensing Mechanism of Carbon Nanotubes: From Single Tubes to High-density Networks. *Carbon* **2014**, *69*, 417–423.

(38) Skakalova, V.; Kaiser, A. B.; Woo, Y.-S.; Roth, S. Electronic Transport in Carbon Nanotubes: From Individual Nanotubes to Thin and Thick Networks. *Phys. Rev. B* **2006**, *74*, 085403.

(39) Peng, N.; Zhang, Q.; Chow, C. L.; Tan, O. K.; Marzari, N. Sensing Mechanisms for Carbon Nanotube Based NH3 Gas Detection. *Nano Lett.* **2009**, *9*, 1626–1630.

(40) Liu, S. F.; Moh, L. C. H.; Swager, T. M. Single-Walled Carbon Nanotube-Metalloporphyrin Chemiresistive Gas Sensor Arrays for Volatile Organic Compounds. *Chem. Mater.* **2015**, 3560–3563.

(41) Feng, X.; Irle, S.; Witek, H.; Morokuma, K.; Vidic, R.; Borguet, E. Sensitivity of Ammonia Interaction with Single-Walled Carbon Nanotube Bundles to the Presence of Defect Sites and Functionalities. *J. Am. Chem. Soc.* **2005**, *127*, 10533–10538.

(42) Zanolli, Z.; Leghrib, R.; Felten, A.; Pireaux, J.-J.; Llobet, E.; Charlier, J.-C. Gas Sensing with Au-Decorated Carbon Nanotubes. *ACS Nano* **2011**, *5*, 4592–4599.

(43) Zhang, T.; Nix, M.; Yoo, B.-Y.; Deshusses, M.; Myung, N. Electrochemically Functionalized Single-Walled Carbon Nanotube Gas Sensor. *Electroanalysis* **2006**, *18*, 1153–1158.

(44) McEuen, P. L.; Fuhrer, M. S.; Park, H. Single-walled Carbon Nanotube Electronics. *IEEE Trans. Nanotechnol.* **2002**, *1*, 78–85.

(45) Collins, P. G.; Bradley, K.; Ishigami, M.; Zettl, A. Extreme Oxygen Sensitivity of Electronic Properties of Carbon Nanotubes. *Science* **2000**, *287*, 1801–1804.

(46) Battie, Y.; Ducloux, O.; Thobois, P.; Dorval, N.; Lauret, J. S.; Attal-Tretout, B.; Loiseau, A. Gas Sensors Based on Thick Films of Semi-conducting Single Walled Carbon Nanotubes. *Carbon* **2011**, *49*, 3544–3552.

(47) Battie, Y.; Gorintin, L.; Ducloux, O.; Thobois, P.; Bondavalli, P.; Feugnet, G.; Loiseau, A. Thickness Dependent Sensing Mechanism in Sorted Semi-conducting Single Walled Nanotube Based Sensors. *Analyst* **2012**, *137*, 2151–2157.

(48) Suehiro, J.; Zhou, G.; Imakiire, H.; Ding, W.; Hara, M. Controlled Fabrication of Carbon Nanotube NO2 Gas Sensor Using Dielectrophoretic Impedance Measurement. *Sens. Actuators, B* **2005**, *108*, 398–403.

(49) Watts, P. C. P.; Mureau, N.; Tang, Z.; Miyajima, Y.; Carey, J. D.; Silva, S. R. P. The Importance of Oxygen-containing Defects on Carbon Nanotubes for the Detection of Polar and Non-polar Vapours through Hydrogen Bond Formation. *Nanotechnology* **2007**, *18*, 175701.

(50) Pingitore, V.; Miriello, D.; Drioli, E.; Gugliuzza, A. Integrated Carboxylic Carbon Nanotube Pathways with Membranes for Voltage-activated Humidity Detection and Microclimate Regulation. *Soft Matter* **2015**, *11*, 4461–4468.

(51) Trzpit, M.; Soulard, M.; Patarin, J.; Desbiens, N.; Cailliez, F.; Boutin, A.; Demachy, I.; Fuchs, A. H. The Effect of Local Defects on Water Adsorption in Silicalite-1 Zeolite: A Joint Experimental and Molecular Simulation Study. *Langmuir* **2007**, *23*, 10131–10139.

(52) Michelis, F.; Bodelot, L.; Bonnassieux, Y.; Lebental, B. Highly Reproducible, Hysteresis-free, Flexible Strain Sensors by Inkjet Printing of Carbon Nanotubes. *Carbon* **2015**, *95*, 1020–1026.

(53) Szanyi, J.; Kwak, J. H.; Peden, C. H. F. The Effect of Water on the Adsorption of NO2 in Na– and Ba- Y, FAU Zeolites: A Combined FTIR and TPD Investigation. *J. Phys. Chem. B* **2004**, *108*, 3746–3753.

(54) Kwak, J. H.; Peden, C. H. F.; Szanyi, J. Non-thermal Plasma-assisted NO x Reduction over Na-Y Zeolites: The Promotional Effect of Acid Sites. *Catal. Lett.* **2006**, *109*, 1–6.

(55) Wang, X.; Hanson, J. C.; Szanyi, J.; Rodriguez, J. A. Interaction of H2O and NO2 with BaY Faujasite: Complex Contraction/Expansion Behavior of the Zeolite Unit Cell. *J. Phys. Chem. B* **2004**, *108*, 16613–16616.

(56) Geng, H.-Z.; Kim, K. K.; So, K. P.; Lee, Y. S.; Chang, Y.; Lee, Y. H. Effect of Acid Treatment on Carbon Nanotube-Based Flexible Transparent Conducting Films. *J. Am. Chem. Soc.* **2007**, *129*, 7758–7759.

(57) Zhou, W.; Vavro, J.; Nemes, N. M.; Fischer, J. E.; Borondics, F.; KamarÃąs, K.; Tanner, D. B. Charge Transfer and Fermi Level Shift in P-doped Single-walled Carbon Nanotubes. *Phys. Rev. B* **2005**, *71*, 205423.

(58) Binions, R.; Davies, H.; Afonja, A.; Dungey, S.; Lewis, D.; Williams, D. E.; Parkin, I. P. Zeolite-Modified Discriminating Gas Sensors. *J. Electrochem. Soc.* **2009**, *156*, J46–J51.

Graphical TOC Entry